

Critical Wetting in the Square Ising Model with a Boundary Field

E. V. Albano,^{1,2} K. Binder,¹ D. W. Heermann,¹ and W. Paul¹

Received December 21, 1989; Final April 11, 1990

The Ising square lattice with nearest-neighbor exchange $J > 0$ and a free surface at which a boundary magnetic field H_1 acts has a second-order wetting transition. We study the surface excess magnetization and the susceptibility of $L \times M$ lattices by Monte Carlo simulation and probe the critical behavior of this wetting transition, applying finite-size scaling methods. For the cases studied, the results are not consistent with the presumably exactly known values of the critical exponents, because the asymptotic critical region has not yet been reached. Implication of our results for critical wetting in three dimensions and for the application of the present model to adsorbed wetting layers at surface steps are briefly discussed.

KEY WORDS: Critical wetting; Ising model; Monte Carlo simulations; finite-size scaling.

1. INTRODUCTION

In a system below its critical point where several phases can coexist the forces exerted by a wall may favor a phase different from the phase occurring in the bulk, and this fact may lead to the formation of a wetting layer at the wall, separated by an interface from the bulk phase. For example, for an Ising ferromagnet with positive magnetization in the bulk in zero bulk field a negative boundary field H_1 at the wall may stabilize a domain with oppositely oriented magnetization at the surface.

While in the "nonwet" state of the wall the thickness of such a wetting layer is microscopically small (i.e., a few lattice spacings in the example of the Ising magnet), changing parameters such as H_1 or the temperature T

¹ Institut für Physik, Johannes-Gutenberg-Universität Mainz, D-6500 Mainz, West Germany.

² Alexander von Humboldt-Fellow. Present and permanent address: INIFTA, Universidad de La Plata, La Plata, Argentina.

of the system, one may encounter a wetting transition, where the thickness of the wetting layer diverges, and it stays infinite throughout the wet region (i.e., the interface between the coexisting phases is no longer “bound” to the wall). Such interface unbinding transitions have attracted much interest recently.^{(1–5), 3} While mean-field theory adequately describes them for systems with long-range forces,⁽²⁾ critical wetting in three-dimensional systems with short-range forces still is a controversial issue.^(6–17) Three space dimensions is the marginal case for the validity of mean-field theory of critical wetting; there is a logarithmic divergence of the thickness of the wetting layer when the transition is approached (associate exponent $\nu_{\perp} = 0$).^(6–8) While the critical exponent is $\nu_{\parallel} = 1$ in mean-field theory, renormalization group theory predicts^(6, 8, 10) very different (nonuniversal) values for ν_{\parallel} . Monte Carlo simulations of critical wetting in the three-dimensional Ising model^(9, 13, 15) seem to differ from these renormalization group predictions, while simulations completely neglecting bulk fluctuations treating the interface in a solid-on-solid (SOS)-like approximation⁽¹⁴⁾ agree better with the renormalization group results. It is not clear as yet, however, where the asymptotic critical region for the various models begins^(11, 14, 15, 17) and whether there is any fundamental difference between wetting in Ising models and in SOS models.

In the present paper, we consider critical wetting for the two-dimensional Ising model, where much more information is available from exact results, and hence a more clear-cut interpretation of Monte Carlo studies should be possible. In particular, the critical boundary field $H_{1c}(T)$ where critical wetting occurs is known from Abraham’s exact solution^(18, 19) as

$$\exp(2J/k_B T) [\cosh(2J/k_B T) - \cosh(2H_{1c}/k_B T)] = \sinh(2J/k_B T) \quad (1)$$

and in addition some exact results on magnetization profiles near the wall in zero bulk field⁽²⁰⁾ and on the correlation lengths ξ_{\parallel} , ξ_{\perp} are available,^(21, 22) which imply for the associated exponents $\nu_{\perp} = 1$ and $\nu_{\parallel} = 2$. The same exponents occur when one uses the solid-on-solid approximation for studying wetting in two-dimensional systems, where the only degrees of freedom characterize the random-walk describing the position of the one-dimensional interface.^(23–26) Also, certain exact results on finite-size scaling are known for this model.^(27, 28)

The exact results do not include the behavior of this wetting transition in the Ising model as a function of the *bulk* field, however. Although one has good reasons to believe that the critical behavior asymptotically is the same as in the SOS model limit, the question remains on the width of the critical region and of establishing the behavior of the model over the full

³ See refs. 1–3 for general reviews on wetting.

parameter range. In this respect, the present Monte Carlo simulations—which are the first Monte Carlo studies of this model—make a contribution. This paper also considers the question of the parameter regions in which this exactly known critical behavior can be extracted from Monte Carlo simulations. Since the latter necessarily consider an $L \times M$ geometry with finite linear dimensions M (parallel to the wall) and L (perpendicular to the wall), a finite-size scaling approach is formulated in Section 2 (previous work has considered $\infty \times L$ geometry⁽²⁷⁾ or $M \times \infty$ geometry⁽²⁸⁾ only). Section 3 describes our numerical results and their interpretation, while Section 4 summarizes our conclusions and discusses possible applications of our results.

2. PHENOMENOLOGICAL FINITE-SIZE SCALING THEORY

For a macroscopically thick system ($L \rightarrow \infty$), the total free energy \mathcal{F} can be split into bulk and surface free energies \mathcal{F}_b , \mathcal{F}_s as follows (see ref. 29 for an introductory review), H being the bulk magnetic field:

$$\mathcal{F}(T, H, H_1, L, M) = \mathcal{F}_b(T, H, M) + \frac{1}{L} \mathcal{F}_s(T, H, H_1, M) \quad (2)$$

In this limit it is only the surface free energy \mathcal{F}_s which becomes singular at the wetting transition. Therefore, we focus on this quantity and its derivatives in the finite-size scaling approach. We thus use the ansatz (2) also for arbitrary finite L , in which case \mathcal{F}_s still may also depend on L explicitly. Denoting the distance from the critical wetting line $H_{1c}(T)$ in the T - H_1 plane by t , we can write the singular part of \mathcal{F}_s as (see also ref. 30)

$$\mathcal{F}_s^{(\text{sing})} = t^{\nu_{\parallel}} \tilde{\mathcal{F}}_s \{ t^{-(\nu_{\parallel} + \nu_{\perp})} H, L t^{\nu_{\perp}}, M t^{\nu_{\parallel}} \} \quad (3)$$

Here $\tilde{\mathcal{F}}_s$ is a scaling function, and limits $L \rightarrow \infty$, $M \rightarrow \infty$, $H \rightarrow 0$, $t \rightarrow 0$ are implied. Of course, the motivation for the last two arguments of $\tilde{\mathcal{F}}_s$ is that M “scales” with ξ_{\parallel} , and L “scales” with ξ_{\perp} ($\xi_{\parallel} \sim t^{-\nu_{\parallel}}$, $\xi_{\perp} \sim t^{-\nu_{\perp}}$). Since the surface is a one-dimensional object in “parallel direction,” hyperscaling implies that $\mathcal{F}_s^{(\text{sing})}(T, H=0, H_1) \sim t^{\nu_{\parallel}}$, for $L \rightarrow \infty$, $M \rightarrow \infty$. The scaling power of H in Eq. (3) then is recognized, noting that the thickness of the wetting layer simply is proportional to the surface excess magnetization defined as⁽²⁹⁾

$$m_s = -(\partial \mathcal{F}_s / \partial H)_{T, H_1} = t^{-\nu_{\perp}} \tilde{m}_s \{ t^{-(\nu_{\parallel} + \nu_{\perp})} H, L t^{\nu_{\perp}}, M t^{\nu_{\parallel}} \} \quad (4)$$

and hence $m_s \sim \xi_{\perp} \sim t^{-\nu_{\perp}}$, as required, and \tilde{m}_s is another scaling function. The surface susceptibility becomes

$$\chi_s = (\partial m_s / \partial H)_{T, H_1} = t^{-\nu_{\parallel} - 2\nu_{\perp}} \tilde{\chi}_s \{ t^{-(\nu_{\parallel} + \nu_{\perp})} H, L t^{\nu_{\perp}} \} \quad (5)$$

with $\tilde{\chi}_s$ a third scaling function. Since the total susceptibility of the system can be written, in analogy to Eq. (2), as

$$\chi = \chi_b + \frac{1}{L} \chi_s \underset{t \rightarrow 0}{\approx} \frac{1}{L} \chi_s \quad (6)$$

where the last approximation is justified by the fact that χ_b is a nonsingular finite constant at the wetting transition, we conclude for the singular part of χ

$$\begin{aligned} \chi^{\text{sing}} &= t^{-(\nu_{\parallel} + \nu_{\perp})} (L t^{\nu_{\perp}})^{-1} \tilde{\chi}_s \{ t^{-(\nu_{\parallel} + \nu_{\perp})} H, L t^{\nu_{\perp}}, M t^{\nu_{\parallel}} \} \\ &\equiv t^{-(\nu_{\parallel} + \nu_{\perp})} \tilde{\chi} \{ t^{-(\nu_{\parallel} + \nu_{\perp})} H, L t^{\nu_{\perp}}, M t^{\nu_{\parallel}} \} \end{aligned} \quad (7)$$

This result shows that the total susceptibility of the system contains information on critical exponents of wetting. Since from sampling fluctuations of the total magnetization χ can be calculated straightforwardly and precisely, we shall make use of Eq. (7) extensively. Thus, we exploit a few consequences of Eq. (7), starting from the fact that we eliminate the scaling powers of t in favor of scaling powers of L keeping only an $L t^{\nu_{\perp}}$ term,

$$\chi^{\text{sing}} = H^{-1} \tilde{\chi} \{ L^{1 + \nu_{\parallel}/\nu_{\perp}} H, L t^{\nu_{\perp}}, M/L^{\nu_{\parallel}/\nu_{\perp}} \} \quad (8)$$

which involves a redefined scaling function. Equation (8) implies a sensible limit for $t=0$, $H \neq 0$: then χ^{sing} should be finite, and considering the limit $L \rightarrow \infty$ at fixed ratio $M/L^{\nu_{\parallel}/\nu_{\perp}} = \text{const}$ and at fixed H , we conclude

$$\chi^{\text{sing}} = H^{-1} \hat{\chi}(M/L^{\nu_{\parallel}/\nu_{\perp}}) \quad (9)$$

Conversely, taking for $t=0$ in Eq. (8) the limit $H=0$ when both L and $M/L^{\nu_{\parallel}/\nu_{\perp}}$ are fixed, again a finite maximum value of χ must be reached, since the system then is finite in all its extensions, and therefore χ cannot be divergent. Thus we conclude for the maximum value of χ (reached for $H=0$, $t=0$)

$$\chi^{\text{max}} \sim L^{1 + \nu_{\parallel}/\nu_{\perp}} \hat{\chi}'(M/L^{\nu_{\parallel}/\nu_{\perp}}) \quad (10)$$

We now specify to the case where on the left boundary of the $L \times M$ film the boundary field is chosen as $-|H_1|$ and at the right boundary it is chosen as $+|H_1|$. Irrespective of the sign of t , we then have a single interface in the system between a domain with positive magnetization and a domain with negative magnetization. However, in the nonwet state this interface can be bound to either the left or to the right boundary. Both situations are completely equivalent. For large L (at fixed M) the magnetization of the total system then basically fluctuates between the

positive and the negative value of the bulk spontaneous magnetization. This macroscopic fluctuation, just as at a first-order transition,⁽³¹⁾ implies that χ^{\max} must be proportional to the "volume" LM of the system. This case is correctly reproduced by requesting that for fixed M and $L \rightarrow \infty$ the scaling function $\hat{\chi}'(z)$ must behave as $\hat{\chi}'(z \rightarrow 0) \sim z$. On the other hand, for fixed L in the limit $M \rightarrow \infty$, the quasi-one-dimensional strip must behave as

$$\chi \sim L\xi_{\parallel} \quad (11)$$

since writing χ as a sum over correlations, $\chi = \sum_{ij} \langle S_i S_j \rangle$, we obtain, after coarse graining over a length L and converting the sum to an integral,⁽³⁰⁾ $\chi \sim L \int_0^{\infty} \exp(-z/\xi_{\parallel}) dz = L\xi_{\parallel}$, making use of the fact that in one-dimensional systems the decay of correlations is a simple exponential function.⁽³⁰⁾ Since for fixed L the value of χ_{\parallel} at $t=0$ saturates at⁽³⁰⁾ $\xi_{\parallel} \sim L^{v_{\parallel}/v_{\perp}}$, Eq. (11) implies $\chi \sim L^{1+v_{\parallel}/v_{\perp}}$, i.e., the scaling function $\hat{\chi}'(z \rightarrow \infty)$ tends to a finite nonzero constant.

Similar arguments can be worked out to discuss m_s further. An alternative form to Eq. (4) is [cf. Eq. (8)]

$$m_s = L\tilde{m}_s \{ L^{1+v_{\parallel}/v_{\perp}} H, Lt^{v_{\perp}}, M/L^{v_{\parallel}/v_{\perp}} \} \quad (12)$$

For $t=0$ and $M/L^{v_{\parallel}/v_{\perp}} = \text{const}$ we conclude in the limit $L \rightarrow \infty$ that

$$m_s \sim H^{-1/(1+v_{\parallel}/v_{\perp})} \hat{m}_s(M/L^{v_{\parallel}/v_{\perp}}) \quad (13)$$

On the other hand, for $t=0$, $H \rightarrow 0$, and keeping both L and $M/L^{v_{\parallel}/v_{\perp}}$ finite, we again conclude that the divergence of m_s is cut off by some finite maximum value

$$m_s^{\max} = L\hat{m}'_s(M/L^{v_{\parallel}/v_{\perp}}) \quad (14)$$

Similar scaling relations could obviously be worked out for the other response functions⁽²⁹⁾ $m_1 = -(\partial\mathcal{F}_s/\partial H_1)_{T,H}$, $\chi_1 = (\partial m_1/\partial H)_{T,H_1}$, and $\chi_{11} = (\partial m_1/\partial H_1)_{T,H}$. This obvious extension is left to the reader.

3. MONTE CARLO RESULTS AND THEIR ANALYSIS

Simulations have been carried out at the multitransputer Meiko Computing Surface at the Institute of Physics at the University of Mainz.⁴ For the Ising Hamiltonian in an $L \times M$ geometry with two free boundaries of

⁴ See refs. 32–35 for a description of this facility and for previous applications to other models.

length M and periodic boundary conditions in the remaining direction (Fig. 1), we have

$$\mathcal{H} = -J \sum_{\langle i,j \rangle} S_i S_j - H \sum_i S_i - H_1 \sum_{i \in \text{left boundary}} S_i - H_L \sum_{i \in \text{right boundary}} S_L \quad (15)$$

Unlike related work in three dimensions,^(9, 13, 15) where $H_L = H_1$ is chosen, we use the boundary condition $H_L = -H_1$. While for $H_L = H_1$ and sufficiently negative, two interfaces will exist for $H > 0$, and for the choice $H_L = -H_1$, a single interface is always expected in the system (Fig. 1). For the case $H_L = H_1$ the situation with two interfaces is stable only for sufficiently large bulk field ($H > H^* \sim 1/L$),^(35, 36) while for $H < H^*$ the stable state has a uniformly negative magnetization. While in three dimensions^(9, 13, 15) the situation in Fig. 1a with two interfaces is sufficiently metastable to allow meaningful computer simulations for $0 < H < H^*$ as well, since the interfacial width increases with M only logarithmically, this

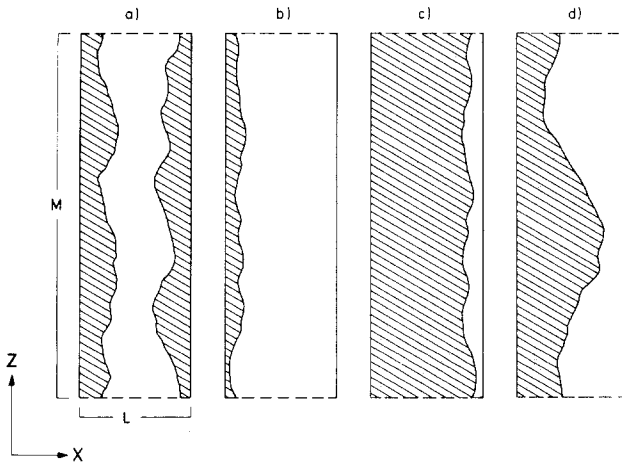


Fig. 1. Simulation geometry indicating schematically the effect of different boundary conditions. Two free boundaries of length M (solid straight lines) and two periodic boundaries of length L (broken straight lines) are used. (a) $H_1 = H_L < 0$; (b)–(d) $H_1 = -H_L < 0$. Regions of positive local (coarse-grained) magnetization are shown as open areas, regions of negative local (coarse-grained) magnetization are shaded, and the interfaces are indicated by solid lines. Cases (b) and (c) refer to the “nonwet” state for bulk field $H = 0$, where a degeneracy occurs with the single interface being “bound” either to the left or to the right boundary, while for the “wet” state [case (d)] the most probable position of the (unbound!) interface is in the center of the strip. By coarse graining we mean an averaging of the local magnetization on the scale of the bulk correlation length to eliminate small clusters of overturned spins, overhangs of the interface, etc.

is not so in two dimensions, where the interfacial width over the length scale M is expected to scale as $M^{1/2}$,⁽⁵⁾ and its local position also relaxes much more rapidly than in three dimensions. With the choice $H_L = -H_1$, and $|H_1|$ sufficiently large, a state with a single interface occurs in thermodynamic equilibrium for arbitrarily small bulk fields. For $H=0$, there is of course a degeneracy between the cases in Figs. 1b and 1c. No sign of the bulk magnetization is preferred. While for large L in the nonwet state the interface is either close to the right (Fig. 1c) or to the left (Fig. 1b) boundary, and hence the average magnetization of the strip is either close to the positive or the negative value of the bulk spontaneous magnetization, the wet state is characterized by an interface position fluctuating around the center of the film, and hence the most probable values of the average magnetization of the strip are close to zero.

Note that in this discussion we assume that M is much less than a characteristic length⁽³⁷⁾ $\xi_d \sim \exp(2\sigma_{\text{int}}L/k_B T)$. If M would exceed this length, for $H=0$ the strip would in the nonwet state be decomposed into a succession of domains of positive and negative magnetization, ξ_d being the average distance between domain walls running perpendicular to the strip, unlike the situations shown in Fig. 1. Near the wetting transition one could also imagine a situation where locally in the strip one crosses over from the situation such as in Fig. 1b to the case of Fig. 1c with the interface making a (seldom) large excursion similar to Fig. 1d. Therefore our simulations cannot be directly interpreted with the theory of Privman and Švrakic,⁽²⁷⁾ where $M \rightarrow \infty$ is considered throughout. Of course, the limit $M \rightarrow \infty$ is more conveniently studied by transfer matrix calculations than by Monte Carlo for $d=2$.

Figure 2 shows snapshots of the actual typical system configurations as observed in our simulations. Extrapolating the positions of the susceptibility maxima of the “susceptibility” χ'

$$k_B T \chi' \equiv \left[\left\langle \left(\sum_i S_i \right)^2 \right\rangle_T - \left\langle \left| \sum_i S_i \right| \right\rangle_T^2 \right] / LM \quad (16)$$

vs. $1/L$, a rough estimation of the wetting critical line H_{1c} has already been performed (Fig. 3).⁽³⁴⁾ There only small values of L ($L \leq 24$) were used. Within the rather modest accuracy of this study, the exact result of Abraham⁽¹⁸⁾ is compatible with the Monte Carlo data; of course, this is a consistency check only. New insight, however, is gained by checking some of the finite-size scaling relations of Section 2, as done in Figs. 4–6. Here also sometimes data on the standard susceptibility [defined as Eq. (16), but without the absolute value sign] $k_B T \chi$ are included.

Figure 4 checks Eq. (10), noting $v_{\parallel} = 2$, $v_{\perp} = 1$, $\chi_{\text{max}}/LM \sim$

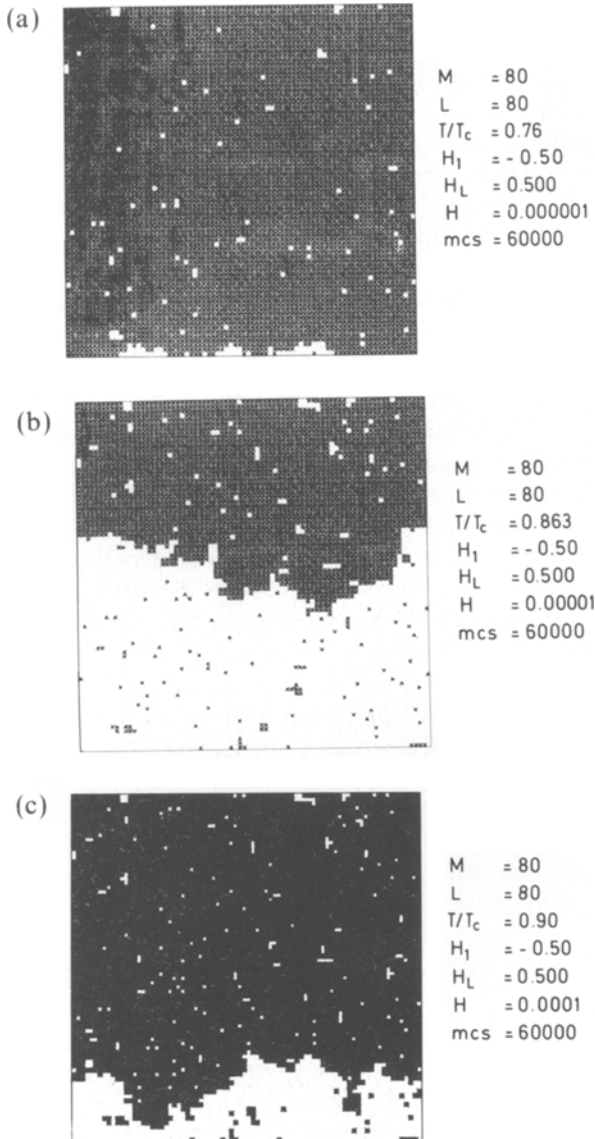


Fig. 2. Snapshots of the spin configuration for $L=80$, $M=80$, $H_1/J=-0.5$, and (a) $H/J=10^{-6}$, $T/T_c=0.76$, (b) $H/J=10^{-5}$, $T/T_c=0.863$, and (c) $H/J=10^{-4}$, $T/T_c=0.9$. Spins $S_i=+1$ are indicated by black stars (thus, unlike Fig. 1, no coarse graining is performed). Time of the snapshots is $t=60,000$ Monte Carlo steps (MCS) per spin, after the system is started from a state with $S_i=-1$ for the x coordinate of the site i being less than or equal to $L/2$ and $S_i=+1$ for the x coordinate of the site i exceeding $L/2$.

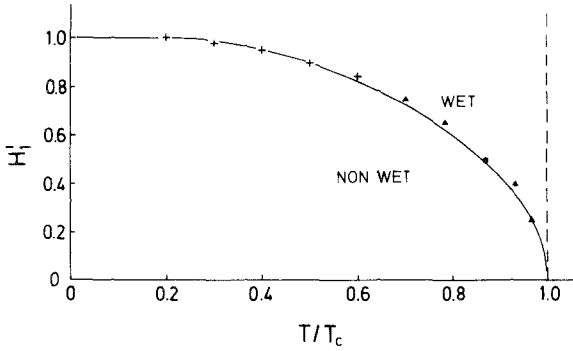


Fig. 3. Wetting phase diagram of the two-dimensional Ising ferromagnet in the plane of variables $H_1' = -H_1/J$ and T/T_c , where T_c is the bulk critical temperature, $k_B T_c/J \approx 2.269$. (—) The exact result of Abraham [Eq. (1)]; (+) results from analyzing the variation of χ' [Eq. (16)] with H_1 at fixed T , (\blacktriangle) from varying T at fixed H_1 , (\bullet) from analyzing the probability distribution of the total strip magnetization.⁽³⁴⁾

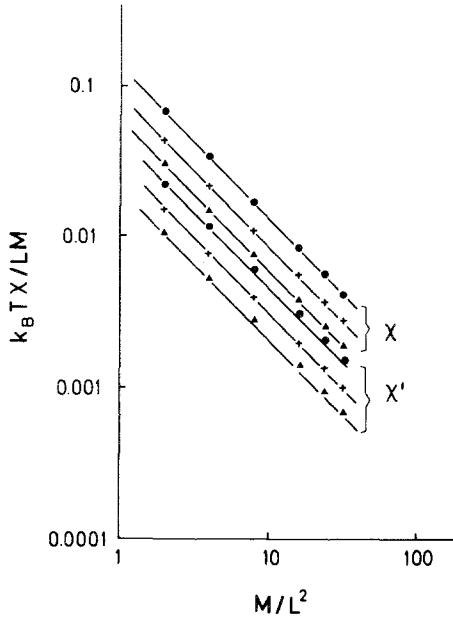


Fig. 4. Log-log plot of $k_B T \chi / LM$ and $k_B T \chi' / LM$ vs. M/L^2 for strips of fixed width $L = 8$ and various M in the range $128 \leq M \leq 1048$, and $T/T_c = (\bullet) 0.863$, $(+) 0.913$, and $(\blacktriangle) 0.963$. All data are for $H_1' = 0.5$ and $H = 0$. Here $T/T_c = 0.863$ is exactly at the wetting transition, and the two other temperatures are in the wet region of the phase diagram, Fig. 3.

$L^2/M\hat{\chi}'(M/L^2) \sim (M/L^2)^{-1}$ for M/L^2 large enough such that $\hat{\chi}'$ can be approximated by its limiting value, $\hat{\chi}'(\infty)$. In the wet region, the same variation is expected as for the wetting transition itself, and this is clearly borne out. These data were obtained from averaging over 6.75×10^5 Monte Carlo steps (MCS) per spin, discarding the initial 0.2×10^5 MCS/spin, using an array of 23 transputer processors working in parallel.

In the regime where the strip is fairly thick, i.e., where the scaling variable $M/L^{v_{\parallel}/v_{\perp}} = M/L^2$ in Eq. (8) is small enough, we find the susceptibility to be nearly independent of this scaling variable, at least within the statistical scatter (Fig. 5). In Fig. 5 we have plotted for $t=0$ ($T/T_c = 0.863$ at $H_1 = 0.5$) the normalized susceptibility $k_B T\chi'/L^3$, which according to Eq. (8) should then be equal to $(HL^3)^{-1}$. This is borne out by the data of Fig. 5.

Figure 6 tests the temperature dependence of χ' as predicted by Eqs. (5) and (6). For large enough L and M off the wetting transition we simply should have $\chi' \sim \chi_s/L \sim t^{-v_{\parallel} - 2v_{\perp}}/L \sim t^{-4}/L$. Our numerical data are consistent with this prediction in the decade $0.03 < t < 0.3$, while closer to the wetting transition, finite-size effects are clearly present, and there is also strong statistical scatter. This strong scatter reflects already the slow motions of the interface, which now is nearly completely "depinned" from the boundary. At and above the wetting transition, the free interface slowly diffuses back and forth across the strip (on a time scale of the order of 10^4 MCS/spin for $L=M=80$; see Fig. 7), and hence for $t \leq 0$ (in the wet regime) it is very hard to take meaningful data on χ' and other thermodynamic quantities.

The magnetization profiles (Fig. 8) can be used to extract both the surface layer magnetization m_1 (Fig. 9a) and the surface excess magnetization m_s (Fig. 9b), since an alternative definition instead of Eq. (4) is expressed in terms of the local magnetization m_l in the l th layer⁽²⁹⁾

$$m_s = \sum_{l=1}^{L/2} (m_b - m_l), \quad L \rightarrow \infty \quad (17)$$

noting that for large l , m_l must approach the bulk magnetization in the film. For the surface layer magnetization, we predict for $T = T_w$ a critical behavior

$$\Delta m_1 \equiv m_1(H) - m_1(0) \sim H^{1 - (v_{\perp} + 1)/(v_{\perp} + v_{\parallel})} = H^{1/3} \quad (18)$$

since from Eq. (4) we find for the layer susceptibility⁽²⁹⁾ $\chi_1 \equiv -(\partial^2 \mathcal{F}_s / \partial H \partial H_1) = \partial m_s / \partial H_1$

$$\chi_1 \sim \left(\frac{\partial m_s}{\partial t} \right)_H = t^{-v_{\perp} - 1} \hat{\chi}_1(t^{-(v_{\perp} + v_{\parallel})} H), \quad L \rightarrow \infty, \quad M \rightarrow \infty \quad (19)$$

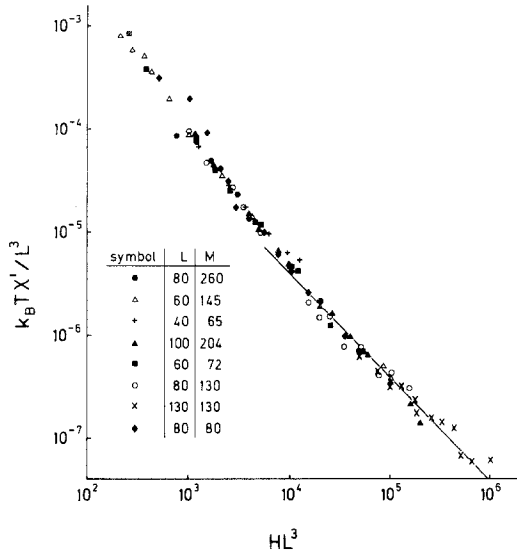


Fig. 5. Scaled susceptibility $k_B T \chi' / L^3$ on a log-log plot vs. HL^3 for $T/T_c = 0.863$, $H_1 = 0$, and various choices of L and M as indicated in the figure. The magnetic field is measured in units of J throughout. Straight line indicates a slope of minus one. Data are based on averages from 10^5 to 7.5×10^5 MCS/site, with 0.2×10^5 initial steps being discarded.

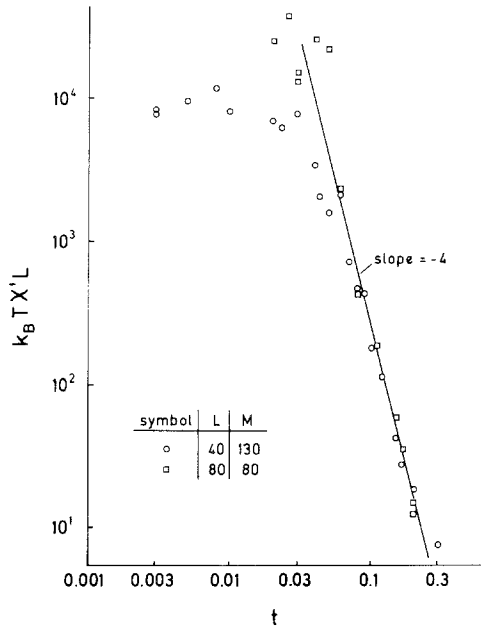


Fig. 6. Normalized susceptibility $k_B T \chi' L$ plotted vs. $t \equiv (T_w - T) / T_c$, where T_w is the wetting critical temperature for $H_1 = 0.5$ [$H_{1c}(T_w) = 0.5$], on a log-log plot.

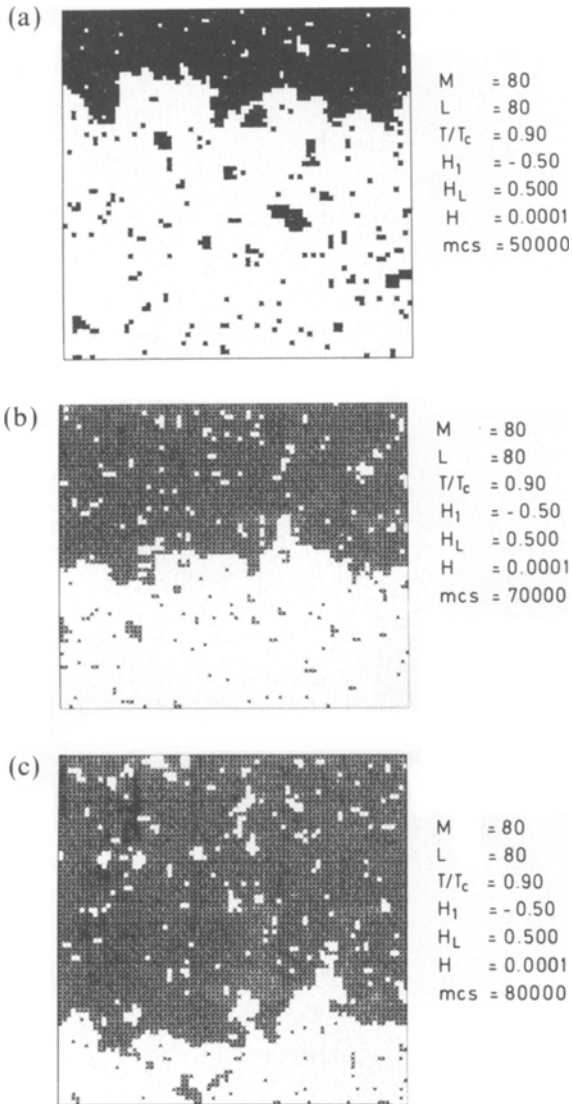


Fig. 7. Snapshots of the spin configuration for $L=80$, $M=80$, $H_1=0.5$, $H/J=10^4$, $T/T_c=0.9$, and different times: (a) $t=5 \times 10^4$ MCS, (b) $t=7 \times 10^4$ MCS, and (c) $t=8 \times 10^4$ MCS. Spins $S_i = +1$ are shown by black stars; spins $S_i = -1$ are not shown.

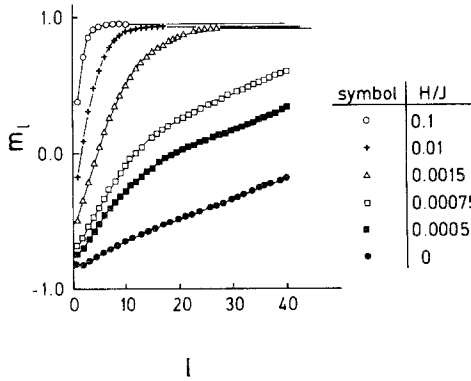


Fig. 8. Magnetization profile m_l vs. layer index l across the strip, for $L = M = 130$, $H'_1 = 0.5$, $T = T_w = 0.863T_c$, and various magnetic fields as indicated in the figure. These results were based on averages over 6.75×10^5 MCS/spin, with the first 2×10^4 being discarded.

where we have interpreted the distance t from the wetting transition as $H_1 - H_{1c}$ for $T = \text{const}$. For $t = 0$, $H \neq 0$, χ_1 must be finite, which in fact is only possible if

$$\hat{\chi}_1(z) \sim z^{(v_\perp + 1)/(v_\perp + v_\parallel)}$$

and therefore

$$\chi_1(t=0) \sim H^{-(v_\perp + 1)/(v_\perp + v_\parallel)}$$

Since the alternative definition for χ_1 is⁽²⁹⁾ $\chi_1 = (\partial m_1 / \partial H)_{H_1, T}$, Eq. (18) follows from integration, $\Delta m_1 = \int_0^H \chi_1 dH$.

From the fact that for small H the slowness of the fluctuations of the interface which then is practically “depinned” from the boundary (Fig. 7) would require much larger computational effort than was available (runs of up to 675,000 MCS/spin were performed for a system size 130×130 , for instance), data for $H/J < 10^{-3}$ had to be discarded. On the other hand, for $H/J > 0.01$, finite-size effects were found to be completely negligible (Fig. 9b). Thus, we have not attempted to test Eq. (14), but rather checked the simple power law [cf. Eq. (13)]

$$m_s \sim H^{-1/(1 + v_\parallel/v_\perp)} = H^{-1/3}, \quad L \rightarrow \infty, \quad M \rightarrow \infty, \quad H \rightarrow 0 \quad (20)$$

Now the surprising feature of our data is that for $0.001 \leq H/J \leq 0.1$, where we feel that statistically significant data are available, Eq. (18) seems to be compatible with the Monte Carlo results (Fig. 9a), while Eq. (20) is not (Fig. 9b). For $H/J \leq 0.01$ the “effective exponent” in Fig. 9b is close to $-\frac{1}{2}$

instead of $-\frac{1}{3}$, but the smooth curvature extending over a wide region in this plot indicated that the asymptotic regime where Eq. (20) holds has not been reached.

To elucidate this problem further, we have also taken data in the regime of “complete wetting” (Fig. 10),⁽³⁸⁾ where $H'_1 > H'_{1c}$. The behavior of m_s is very similar; over the regime $0.001 \leq H/J \leq 0.1$, the $\log m_s$ vs. $\log H$ plot is curved, and for the smallest fields the onset of finite-size effects is masked by strong statistical scatter. However, the variation of Δm_1 with H for small H now is simply analytic, reflecting a finite value of χ_1 for the wet regime, as expected from the analogous results in $d=3$ dimensions.^(13, 15)

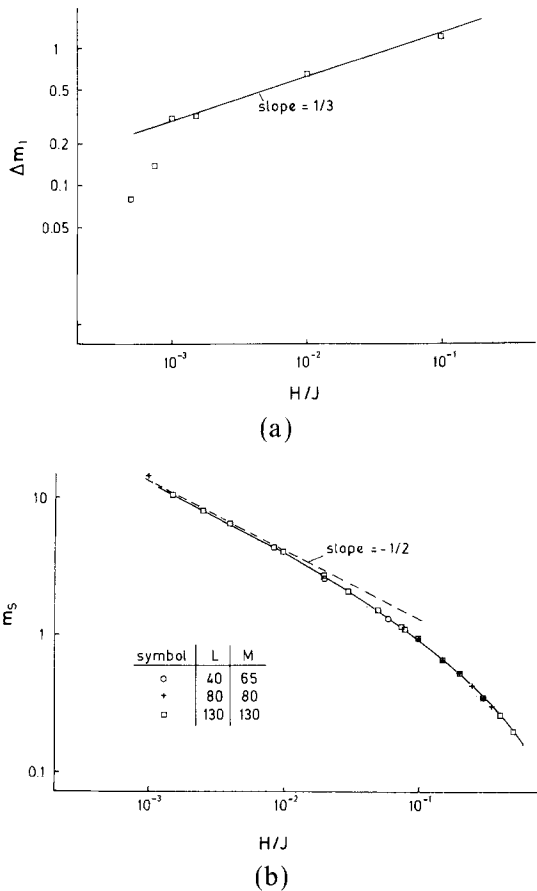
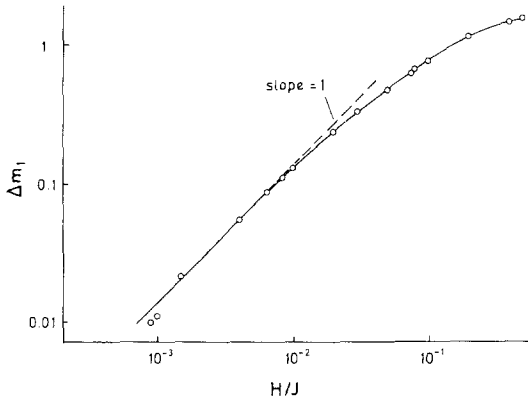
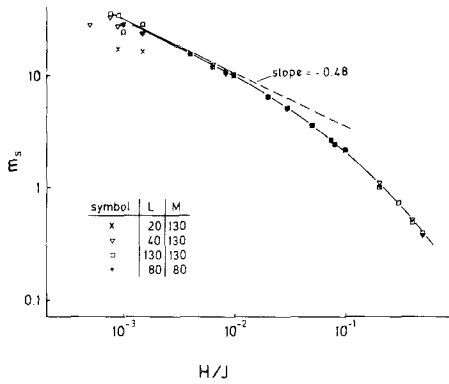


Fig. 9. Log-log plot of (a) Δm_1 and (b) m_s vs. magnetic field, for $H'_1 = 0.5$ and $T = T_w = 0.863T_c$. In case (b) also additional smaller sizes $L \times M$ are included as indicated in the figure.



(a)



(b)

Fig. 10. Same as Fig. 9, but for $H'_1 = 0,8$, $T = 0.863T_c$. Linear dimensions for case (a) are $L = M = 80$.

4. DISCUSSION

In this paper a Monte Carlo study of critical and complete wetting in two dimensions has been presented, and the results have been interpreted in terms of various theories. While for bulk field $H=0$ the model has been solved exactly by Abraham,⁽¹⁸⁻²²⁾ and thus the location of the critical wetting line is exactly known (Fig. 3), the behavior for nonzero field can only be inferred from scaling assumptions. Thus, the purpose of our Monte Carlo study has been twofold. Comparison with exactly known critical

exponents gives information on the width of the critical region for the second-order wetting transition in this model. In the analogous three-dimensional Ising model, this is a debated issue. Furthermore, one can check that the limitations of every Monte Carlo simulation, namely finite-averaging time effects and finite-size effects, are well under control in this model. This fact is rather nontrivial, since the interfacial fluctuations are very slow (see Fig. 7 for an illustration), and the finite-size effects are quite nontrivial, since the correlation lengths ξ_{\parallel} , ξ_{\perp} diverge with rather different (and large!) exponents, namely $\nu_{\parallel} = 2$, $\nu_{\perp} = 1$. Thus, one expects that for $t = 10^{-1}$ the correlation length ξ_{\parallel} may already be of the order of 10^2 , which implies that the computational task is rather demanding. In addition, the finite-size scaling analysis is rather tricky, as should be obvious from Section 2, where the appropriate background theory has been worked out. In our case, the analysis is of course somewhat facilitated by the fact that the location of the critical wetting transition was used throughout—anisotropic models where neither T_c nor the critical exponents are understood, as in the driven Kawasaki model, and its variants are still much less under control when one applies analogous methods.^(30, 39) Therefore, the present model is a useful testing ground for the application of Monte Carlo techniques to models with anisotropic critical behavior. Finally, the predictions of the scaling theory for describing the effects of the bulk field on the wetting transition and on the wet phase can be tested.

Given these expectations, not all of our results are clear-cut. While the thermal variation of χ' seems to be consistent with theory already very far from the transition ($0.03 < t < 0.3$), the predicted variation of the surface excess magnetization with bulk magnetic field, Eq. (20), has not been verified for the accessible regime of fields, $H/J > 10^{-3}$. In this regime, m_s is of the order of 10 (Fig. 9b) or larger (Fig. 10b), and thus the reason for the narrowness of the critical region is not understood. On the other hand, the relation $\Delta m_1 \sim H^{1/3}$ has been verified (Fig. 9a). The situation is exactly opposite to the three-dimensional case,^(13, 15) where the theoretical relation m_s vs. $H(m_s \sim \ln H$ in this case) is nicely established, while the Δm_1 vs. H relation is not. It is hoped that our observations will stimulate additional theoretical activity to explain these findings.

While some of the predictions from finite-size scaling for the surface susceptibility could be verified (see Figs. 4 and 5), a larger part of these predictions remains untested, because statistically significant Monte Carlo data could not yet be generated with affordable effort. Part of our calculations have been performed on the parallel computer described in ref. 32, where four transputers work in parallel, while the larger fraction has been generated on a MEIKO Computing Surface containing 80 transputers, out of which a domain of 23 transputers was used for the present calculations.

In the latter case a performance of 10^7 spin flip trials per second was reached. Since linear dimensions L , M of the order of 10^2 certainly are required to ensure that the asymptotic regime of validity for finite-size scaling is reached, and then the relaxation time for interfacial fluctuations is at least of the order of 10^4 in the wet regime, a substantial amount of CPU time is clearly required to proceed further.

Finally, we again draw attention to the fact that the present model should be relevant to adsorption at stepped surfaces in the submonolayer coverage range.⁽³³⁻³⁵⁾ The boundary field H_1 then accounts for "missing neighbors" of adatom absorbed right next to a step, and possibly to a change in its binding energy. The bulk magnetic field translates into the chemical potential difference between high-density and low-density phases adsorbed at a perfect flat substrate surface of infinite extent. The magnetization profile would then correspond to the coverage profile in the direction perpendicular to the step. Again in this case a finite distance L between steps (and another finite distance M over which the "terrace" between steps in the direction parallel to the steps is ideal) is physically more plausible than the perfectly infinite system $L \rightarrow \infty$, $M \rightarrow \infty$, and hence the phenomenological theory of Section 2 finds another application there.

ACKNOWLEDGMENTS

One of us (E.V.A) thanks the Alexander von Humboldt foundation for support through a research fellowship and the Consejo Nacional de Investigaciones Cientificas y Tecnicas de la Republica Argentina for support. This work also was supported by the BAYER AG, Leverkusen, and the Bundesministerium für Forschung und Technologie (BMFT) under grant 03M4028.4.

REFERENCES

1. D. E. Sullivan and M. M. Telo da Gama, in *Fluid Interfacial Phenomena*, C. A. Croxton, ed. (Wiley, New York 1986).
2. S. Dietrich, in *Phase Transitions and Critical Phenomena*, Vol. XII, C. Domb and J. L. Lebowitz, eds. (Academic, New York, 1988), p. 1.
3. E. H. Hauge, in *Fundamental Problems in Statistical Physics VI*, E. G. D. Cohen (North-Holland, Amsterdam, 1985), p. 65.
4. W. Selke, D. A. Huse, and D. M. Kroll, *J. Phys. A* **17**:3019 (1984).
5. P. G. de Gennes, *Rev. Mod. Phys.* **55**:825 (1985); M. E. Fisher, *J. Chem. Soc. Faraday Trans. 2* **82**:1569 (1986); *J. Stat. Phys.* **34**:667 (1984).
6. E. Brézin, B. I. Halperin, and R. K. P. Zia, *Phys. Rev. Lett.* **50**:1387 (1983).
7. R. Lipowsky, D. M. Kroll, and R. K. P. Zia, *Phys. Rev. B* **27**:4499 (1983).

8. D. S. Fisher and D. A. Huse, *Phys. Rev. B* **32**:247 (1985).
9. K. Binder, D. P. Landau, and D. M. Kroll, *Phys. Rev. Lett.* **56**:2276 (1986).
10. R. Lipowsky and M. E. Fisher, *Phys. Rev. B* **36**:2126 (1987); *Phys. Rev. Lett.* **57**:2411 (1986).
11. E. Brézin and T. Halpin-Healey, *Phys. Rev. Lett.* **58**:1220 (1987).
12. E. Brézin and T. Halpin-Healey, *J. Phys. (Paris)* **48**:757 (1987).
13. K. Binder and D. P. Landau, *Phys. Rev. B* **37**:1745 (1988).
14. D. M. Kroll, *J. Appl. Phys.* **61**:3595 (1988); G. Gompper and D. M. Kroll, *Phys. Rev. B* **37**:529 (1988).
15. K. Binder, D. P. Landau, and S. Wansleben, *Phys. Rev. B* **40**:6971 (1989).
16. A. D. Parry and R. Evans, *Phys. Rev. B* **39**:12336 (1989).
17. T. Halpin-Healey, *Phys. Rev. B* **40** (1989).
18. D. B. Abraham, *Phys. Rev. Lett.* **44**:1165 (1980).
19. D. B. Abraham, in *Phase Transitions and Critical Phenomena*, Vol. X, C. Domb and J. L. Lebowitz, eds. (Academic, New York, 1987), p. 1.
20. D. B. Abraham and D. A. Huse, *Phys. Rev. B* **38**:7169 (1988).
21. D. B. Abraham and E. R. Smith, *J. Stat. Phys.* **43**:621 (1986).
22. D. B. Abraham, *J. Phys. A* **21**:1741 (1988).
23. S. T. Chui and J. D. Weeks, *Phys. Rev. B* **23**:2438 (1981).
24. T. W. Burkhardt, *J. Phys. A* **14**:L63 (1981).
25. D. M. Kroll, *Z. Phys. B* **41**:345 (1981).
26. J. M. J. van Leeuwen and H. J. Hilhorst, *Physica A* **107**:319 (1981).
27. V. Privman and N. M. Švrakic, *Phys. Rev. B* **37**:3713 (1988).
28. D. M. Kroll and G. Gompper, *Phys. Rev. B* **39**:433 (1989).
29. K. Binder, in *Phase Transitions and Critical Phenomena*, Vol. VIII, C. Domb and J. L. Lebowitz, eds. (Academic, New York, 1983), p. 1.
30. K. Binder and J. S. Wang, *J. Stat. Phys.* **55**:87 (1989).
31. K. Binder and D. P. Landau, *Phys. Rev. B* **30**:1477 (1984).
32. D. W. Heermann and R. C. Desai, *Computer Phys. Commun.* **50**:536 (1988); R. C. Desai, D. W. Heermann, and K. Binder, *J. Stat. Phys.* **53**:795 (1988).
33. E. V. Albano, K. Binder, D. W. Heermann, and W. Paul, *Z. Phys. B* **77**:445 (1989).
34. E. V. Albano, K. Binder, D. W. Heermann, and W. Paul, *Surf. Sci.* **223**:151 (1989).
35. E. V. Albano, K. Binder, D. W. Heermann, and W. Paul, *J. Chem. Phys.* **91**:3700 (1989).
36. M. E. Fisher and H. Nakanishi, *J. Chem. Phys.* **75**:5857 (1981); H. Nakanishi and M. E. Fisher, *J. Chem. Phys.* **78**:3279 (1983).
37. M. E. Fisher, *J. Phys. Soc. Japan Suppl.* **26**:87 (1969); see also G. G. Cabrera, R. Jullien, E. Brézin, and J. Zinn-Justin, *J. Phys. (Paris)* **47**:1305 (1986).
38. R. Lipowsky, *Phys. Rev. B* **32**:173 (1985).
39. J. S. Wang, K. Binder, and J. L. Lebowitz, *J. Stat. Phys.* **56**:783 (1989).